Journal of Laser Applications

Influence of ultrasonic amplitude and position in the vibration distribution on the microstructure of a laser beam welded aluminum alloy

Cite as: J. Laser Appl. **31**, 022402 (2019); https://doi.org/10.2351/1.5096100
Submitted: 14 March 2019 . Accepted: 14 March 2019 . Published Online: 09 April 2019

Sarah Nothdurft, Hendrik Ohrdes, Jens Twiefel, Jörg Wallaschek, Maximilian Mildebrath, Hans Jürgen Maier, Thomas Hassel, Ludger Overmeyer, and Stefan Kaierle

Journal of Laser Applications ARTICLE scitation.org/journal/jla

Influence of ultrasonic amplitude and position in the vibration distribution on the microstructure of a laser beam welded aluminum alloy

Cite as: J. Laser Appl. **31**, 022402 (2019); doi: 10.2351/1.5096100
Submitted: 14 March 2019 · Accepted: 14 March 2019 ·
Published Online: 9 April 2019

Sarah Nothdurft,[1] Hendrik Ohrdes,[2] Jens Twiefel,[2] Jörg Wallaschek,[2] Maximilian Mildebrath,[3] Hans Jürgen Maier,[3] Thomas Hassel,[3] Ludger Overmeyer,[1] and Stefan Kaierle[1]

AFFILIATIONS

[1]Laser Zentrum Hannover e.V., Hollerithallee 8, Hannover 30419, Germany
[2]Institut für Dynamik und Schwingungen, Appelstraße 11, Hannover 30167, Germany
[3]Institut für Werkstoffkunde, An der Universität 2, Garbsen 30823, Germany

Note: This paper is part of the Special Collection: Proceedings of the International Congress of Applications of Lasers & Electro-Optics (ICALEO® 2018).

ABSTRACT

There are many reasons for influencing the laser beam induced weld pool. The manipulation of the dynamics, the solidification, the resulting grain size, and in the end, as a result of the aforementioned influencing, the mechanical characteristics of the weld is the aim of different attempts to gain an impact on the melt. Aluminum alloys tend to porosity formation because of different solubility of hydrogen in solid and liquid states. For reliable welds, the porosity has to be limited. An ultrasound excitation is one possibility to allow a fast degassing, especially for the considered round bars, for which no welding through is possible for geometric reasons. The presented research shows the influence of the ultrasonic amplitude on the microstructure of laser beam welded round bars of the aluminum alloy AA6082-T6. Furthermore, the position of the weld pool in the vibration distribution is varied and the influence evaluated. Metallographic cross sections show in analyses the resulting weld characteristic and the microstructure of the weld metal. The grain size and the grain orientation are evaluated for the different ultrasound parameters. Additionally, the summed porosity area is compared to acquire knowledge about the correlation between ultrasound excitation (with regard to vibration amplitude and position in the vibration distribution) and pore formation.

Key words: laser beam welding, aluminum alloy, ultrasound, microstructure, porosity

 https://doi.org/10.2351/1.5096100

I. INTRODUCTION

There is a wide selection of aluminum alloys for each purpose and according to diverse processing or treatment. Aluminum alloys have many advantages, e.g., low densities for lightweight construction. Furthermore, these materials are characterized by easy mechanical processing, corrosion resistance due to the durable and self-repairing surface layer, and good formability.

Disadvantages are the tendencies toward pore or hot crack formation, a necessary adaption of the component geometry caused by lower strength in comparison to, e.g., steel, a low absorption due to high reflection in solid state and a high heat conduction rate that increases the energy input required.

II. MOTIVATION

For welding aluminum alloys, the risk of porosities in the weld metal occurs primarily because of the strongly different hydrogen solubility for the solid and liquid states.[1] As aluminum alloys are popular structural materials, the demand for reliable high-quality joints is given.

With the use of an x-ray transmission imaging system, the real time observation of keyhole, bubbles, and resulting porosity for high power CO_2 laser beam welding of AA5083 (3.3547) was possible.[2] The formation of porosities (large spherical, elongated, and spikelike root porosities) was shown and the mechanism was explained. Higher welding speeds cause higher amounts of porosities but with

smaller pore diameters, full penetration welding avoids porosities and welding with following laser beam reduces porosities for partial penetration welding.[2]

The impact of vibration on the solidification characteristics of metals is known. Grain refinement for casting processes is already achievable for low frequencies below 100–200 Hz, there is a dependency from the relation between amplitude and frequency. In addition, homogeneity, reduction of microsegregations, improved mechanical characteristics, and financial advantages by redesignable casting molds result.[3]

For expendable pattern shell casting of A356 (3.2371) aluminum alloy with an optimum of 100 Hz, a change in the microstructure is observable.[4] The structure is more dimple instead of coarse structures, resulting in a higher ductility, tensile strength, yield strength, elongation, and hardness.[4]

The simultaneous liquid area is much smaller for welding processes than for casting processes. For arc welding with 20 kHz and an amplitude of 10 μm aluminum alloys show a higher weld depth, a better weld quality with regard to porosities and hardness of the heat affected zone, the shielding gas protection is restricted, and precipitation of silicon and copper has been observed.[5] For tungsten inert gas welding of AA7075 (3.4365), an electric transducer can be used to reduce hot cracking and to improve the microstructure (grain size and shape) as well as hardness values.[6] Best results were obtained, when a frequency of above 2 kHz is introduced.

The question arises whether a similar effect is obtainable for laser beam welding with its typically high solidification speeds.

A reduction of porosity, as well as hardness in the heat affected zone, is achieved for pulsed laser beam welding with 10 kHz vibration introduced with a piezoelectric transducer.[7] A better aspect ratio and a higher penetration depth can be achieved.

Mechanical vibrations in audible frequencies were investigated with regard to full penetration welding of AA5083 with frequencies between 4 and 12 kHz and show a change of the grain formation from columnar to equiaxed, but the percentage of equiaxed grains seems to be independent of the frequency.[8,9] Furthermore, a connection between the frequency amplitude product as given for vibration stimulation for casting processes[3] could not be proven for laser beam welding.[8] The grain size varies over the weld depth, the smallest grain size in the center of the weld is achieved for frequencies between 2 and 3 kHz, and it seems that amplitudes of 1 μm already affect the grain structure.[9] It is indicated that the vibrations can change the fluid flow in the melt pool. For laser beam welded dissimilar steel–steel joints, the effect of ultrasonic amplitude on the weldability in regard to hot crack susceptibility was already shown.[10]

III. EXPERIMENTAL SETUP

A. Laser beam welding setup

The laser beam source used for the welding tests was a diode-pumped, solid state disk laser (Trumpf TruDisk 16002), with a maximum output power of 16 kW and a wavelength of 1030 nm. The high power welding head (Precitec YW52) with a collimation length f_C of 150 mm and a focal length f_F of 300 mm is guided by a robot system and creates by using a fiber with a diameter of 200 μm a focal spot diameter of 400 μm. The welding speed is initiated by the motor of the system for the ultrasonic assisted laser beam welding process. The experimental setup is shown in Fig. 1.

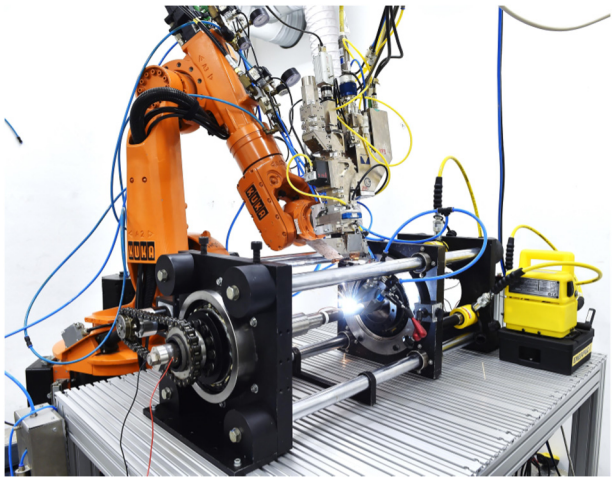

FIG. 1. Experimental setup for the ultrasound assisted laser beam welding.

B. Ultrasonic system

The ultrasonic system is designed to excite the workpieces at approximately 20 kHz. Thereby, the workpieces are part of the vibration system. The workpieces are clamped by a hydraulic system to prevent it from clattering due to dynamic forces. The transducers current amplitude and phase are controlled by the DPC500/100k,[11,12] which was developed at the Institute of Dynamics and Vibration Research. For bead on plate welds, the position in the vibration distribution can be adapted by moving the welding head to the desired position. To identify the vibration maximum (antinode) and the vibration minimum (node), the velocity along the workpieces is measured with a fiberoptic laser vibrometer in in-plane configuration, which allows one to measure the longitudinal vibration velocity. If the workpieces are of equal material and dimension, the vibration distribution along the workpieces can also be calculated, which leads to the longitudinal vibration distribution shown in Fig. 2. Additionally, the dependency between the driving current and the amplitude at the antinode is measured. Based on these measurements, the vibration

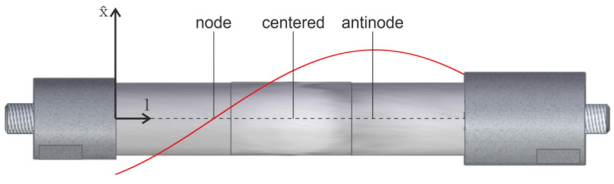

FIG. 2. Calculated vibration distribution based on measurements of the node and antinode positions.

amplitude and stress at every point can be calculated from the driving current.

IV. EXPERIMENTAL PROCEDURE

All bead on plate welding tests were performed on round bars of the aluminum alloy AA6082 (3.2315) with a diameter of 30 mm and a length of 50 mm. Three samples (cf. Fig. 2) were clamped for each test. Three different positions in the waveform of the vibration distribution and three different ultrasound amplitudes were examined. The amplitudes were measured in the point of the destinated weld zone with a laser vibrometer. Figure 2 shows the distribution of the vibration and the selected positions for the welding tests.

The welding parameters are a laser beam power P_L of 6.5 kW and a welding speed v_F of 1.5 m/min. There is an angle of incidence of 10° for the beam to avoid damage of the optical system by back reflection, which can occur for laser beam welding of aluminum alloys. The samples are clamped with a hydraulic pressure of 110 bar. The focal z-position is 4 mm below the surface. The parameters of the samples 0 and A–G are listed in Table I. Each parameter configuration is repeated three times for statistical confidence. In addition, samples with parameter 0 were made for a comparison with the weld characteristics without ultrasonic excitation as a reference. For the node position, controlled and stable vibration amplitudes of 4 and 6 μm were not possible.

Metallographic cross and longitudinal sections were prepared for each sample. The pore area is measured for prepared cross/longitudinal sections without etching, the weld geometry is analyzed with electrolytically polished samples according to Barker (25 V, 0.1 A, 120 s, 700 ml H_2O + 30 ml HBF_4), also the grain size is detected. Furthermore, x-ray photographs (Seifert ISOVOLT 320, 80 kV, 20 mA, 3.6 min) were taken for selected parameter configurations (three samples per parameter).

The weld width, weld depth, weld metal area, pore area, and grain size were identified and evaluated. The results of the measurements and estimations are discussed in Sec. V.

V. RESULTS AND DISCUSSION

In Fig. 3, top view photographs of the welds are shown exemplarily. The shape of the weld reinforcement is strongly influenced by the ultrasonic excitation. The sagging in the middle is growing with increasing amplitude (vertical) and with position from node to antinode (horizontal).

TABLE I. Parameter configurations.

Sample	v_F (m/min)	P_L (kW)	Position in the vibration distribution	Ultrasound amplitude (μm)
0	1.5	6.5	—	0
A			Node	2
B			Centered	2
C			Centered	4
D			Centered	6
E			Antinode	2
F			Antinode	4
G			Antinode	6

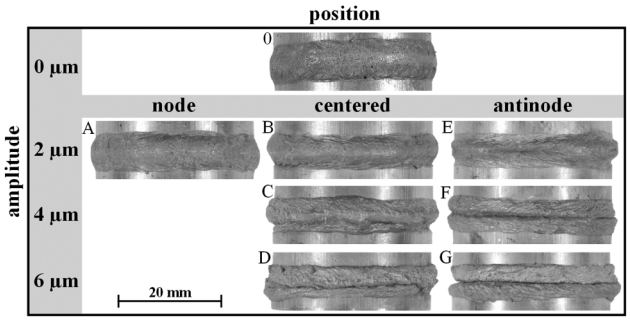

FIG. 3. Photographs of the top view: exemplary for each parameter configuration.

Micrographs of metallographic cross sections also show the shape of the weld reinforcement and confirm its dependency on position and amplitude (cf. Fig. 4).

The ultrasonic excitation has a huge influence on the weld characteristics (weld depth and width). The weld depth (cf. Fig. 5) decreases with increasing amplitude and the weld width (cf. Fig. 6) increases with increasing position. The overall shape of the weld is changing with increasing amplitude from nail shape with width/depth ratio 0.56 (amplitude of 2 μm) to a nearly even ratio of 0.84 (amplitude of 6 μm) for antinode position (cf. Fig. 7).

The influence of position and amplitude on the weld metal area is rather small (cf. Fig. 8).

Furthermore, the grain size and the distribution of the grain size in the weld metal are apparent in the electrolytically polished metallographic cross sections. For higher amplitudes, the grain size is more homogeneous and smaller in general. Also, the position shows a grain refinement for moving from node to antinode. In particular, in the upper area of the weld, the grain size decreases due to the vibrations influence. The last area which is affected seems to be the edges of the middle area.

For more details on the effects of amplitude and position of the vibration distribution, both will be analyzed separately in the following parts.

A. Influence of the amplitude

For the investigation of the influence of the ultrasound amplitude on welding aluminum alloy bead on plate welds, samples 0–B–C–D (centered position, cf. Fig. 9) and 0–E–F–G (antinode position, cf. Fig. 10) are compared.

For the centered position, the weld depth first increases with applied vibration and then there is a decrease for increasing amplitude, whereas the weld width decreases more slightly (cf. Fig. 11, right). Therefore, the width/depth ratio increases for nearly 0.1 for each 2 μm amplitude growth. The weld metal area is constant and does not appear to be dependent on amplitude and position (cf. Fig. 11, left).

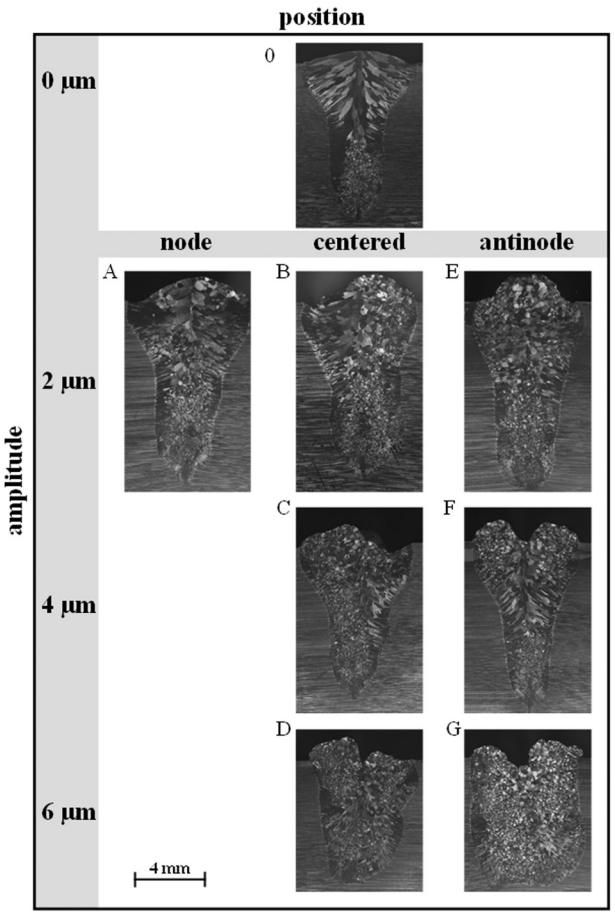

FIG. 4. Micrographs of electrolytically polished cross sections: exemplary for each parameter configuration.

The weld reinforcement decreases and creates sagging between the amplitude of 4 μm and the amplitude of 6 μm. Also, the shape of the weld changes between these amplitudes.

For the antinode position, the weld depth and width behave like in the centered position (cf. Fig. 12, right). The width/depth

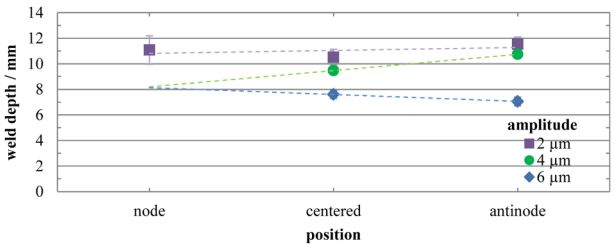

FIG. 5. Correlation between amplitude, position, and weld depth.

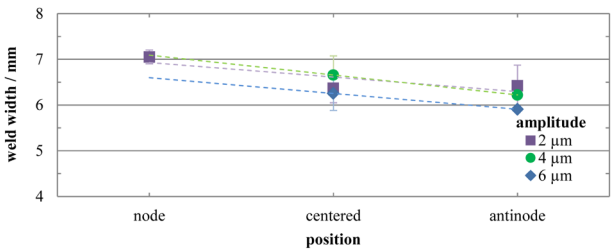

FIG. 6. Correlation between amplitude, position, and weld width.

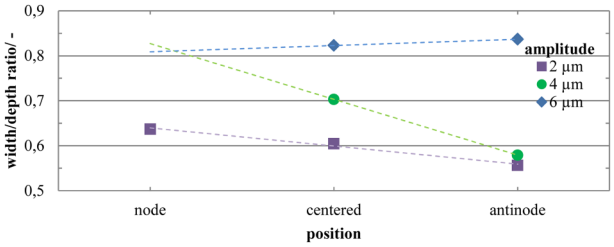

FIG. 7. Correlation between amplitude, position and weld width/depth ratio.

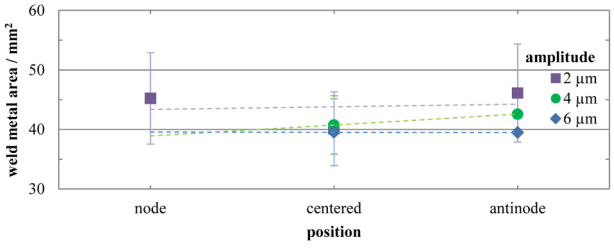

FIG. 8. Correlation between amplitude, position, and weld metal area.

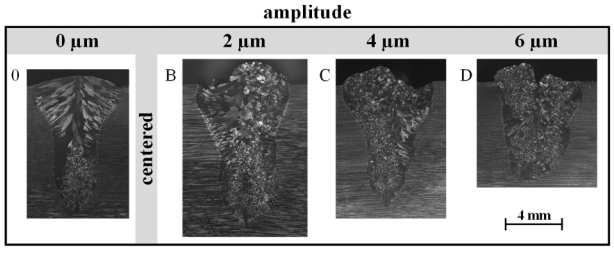

FIG. 9. Micrographs of metallographic cross sections: comparison of exemplary samples for centered position.

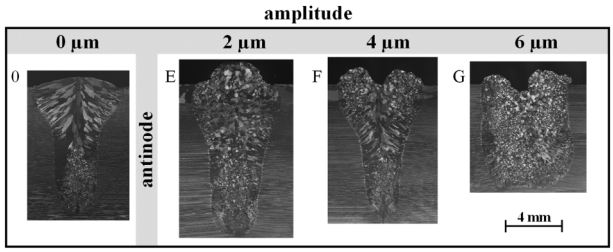

FIG. 10. Micrographs of metallographic cross sections: comparison of exemplary samples for antinode position.

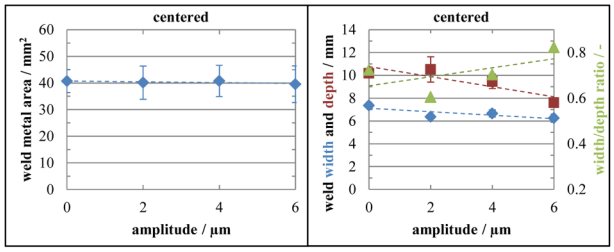

FIG. 11. Correlation between amplitude and weld metal area (left), weld width, weld depth, and width/depth ratio (right) for centered position.

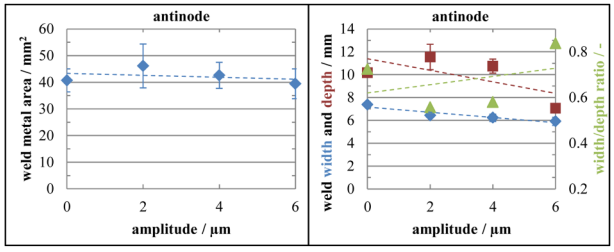

FIG. 12. Correlation between amplitude and weld metal area (left), weld width, weld depth and width/depth ratio (right) for antinode position.

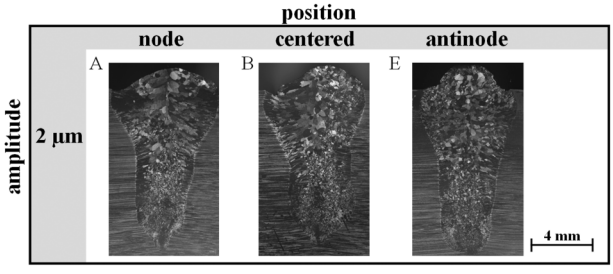

FIG. 13. Micrographs of metallographic cross sections: comparison of exemplary samples with an amplitude of 2 μm.

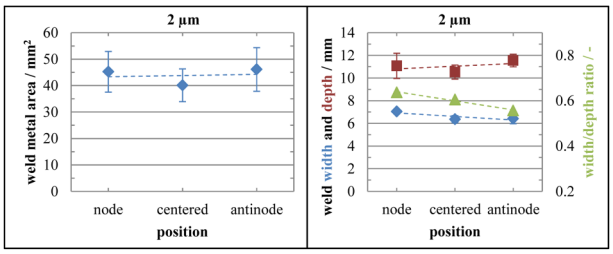

FIG. 14. Correlation between position and weld metal area (left), weld width, weld depth and width/depth ratio (right) for an amplitude of 2 μm.

ratio increase is not as pronounced as shown before. The weld metal area consistency is given (cf. Fig. 12, left).

Therefore, the weld metal area is just the result of the energy input by the laser beam welding process. Weld reinforcement and sagging show a similar behavior compared to the centered position.

The change in the weld shape can be explained by an interference between the keyhole and the vibration or its influence on the weld pool dynamics. It is not possible to keep the keyhole in the area of the weld root open, so the keyhole collapses partly and the weld depth decreases.

B. Influence of the position in the vibration distribution

The influence of the position in the vibration distribution was investigated by comparing samples A–B–E (amplitude of 2 μm, cf. Figs. 13 and 14), C–F (amplitude of 4 μm, cf. Figs. 15 and 16), and D–G (amplitude of 6 μm, cf. Figs. 17 and 18).

For the samples with an amplitude of 2 μm, there is no significant change in the weld geometry. The weld metal area is constant, the weld depth just slightly increases and the width decreases also slightly, but to a greater extent, so the width/depth ratio decreases as conclusion (Fig. 14, right).

For the samples with an amplitude of 4 μm, there is a larger decrease of the weld depth for the movement from antinode to centered position and due to that in the increase of the width/depth

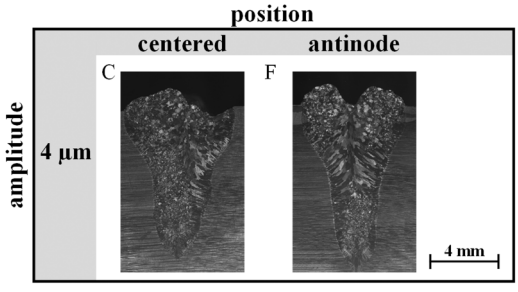

FIG. 15. Micrographs of metallographic cross sections: comparison of exemplary samples with an amplitude of 4 μm.

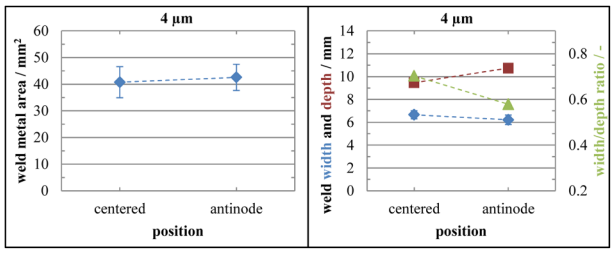

FIG. 16. Correlation between position and weld metal area (left), weld width, weld depth and width/depth ratio (right) for an amplitude of 4 μm.

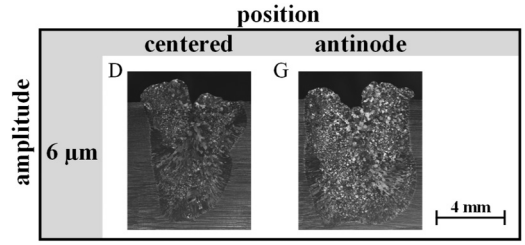

FIG. 17. Micrographs of metallographic cross sections: comparison of exemplary samples with an amplitude of 6 μm.

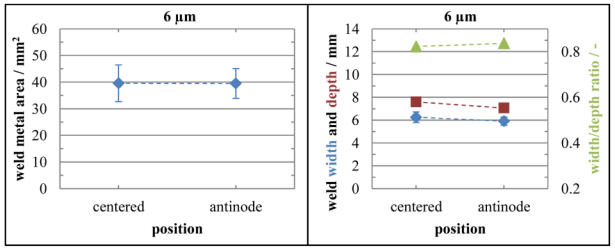

FIG. 18. Correlation between position and weld metal area (left), weld width, weld depth and width/depth ratio (right) for an amplitude of 6 μm.

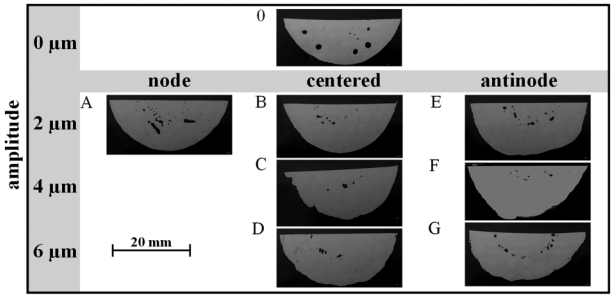

FIG. 19. Micrographs of longitudinal sections: exemplary for each parameter configuration.

ratio. Also, a change in the weld geometry is visible. In the middle of the weld, reinforcement sagging occurs. The weld metal area and the width show a consistent behavior.

For samples with an amplitude of 6 μm, the weld shape is changed for both positions compared to an amplitude of 2 and 4 μm. The weld metal area, depth, width, and width/depth ratio are constant. As a conclusion, the weld characteristics seem to reach a threshold (for the applied welding parameters) and are not affected anymore by a variation of the position.

C. Pore formation

In micrographs of metallographic longitudinal sections prepared without etching, the porosity is clearly visible (Fig. 19). Taking into consideration that only a snapshot of one layer is visible, any amplitude and position lead to smaller and more spread pores. For the highest amplitude in antinode position, the pores form a seam on the bottom of the weld root. The degassing seems to be inhibited, and the gas is trapped in the solidifying metal.

The pore formation is better visible with transmission methods, which are able to map the whole volume. In a comparison between node (A) and centered position (B) for an amplitude of 2 μm, also regarding a sample without amplitude (0), a movement of the pores more to the middle of the sample is detectable (cf. Fig. 20). This means that the formation of pores is transferred to the root of the weld and the pores are not able to leave the point of formation in the surface direction, because of the ultrasonic amplitude.

This would mean that the pore area is bigger for the centered position between node and antinode. To verify this assumption, the pore area was measured. Figure 21 shows the results of the pore area measurement from the photographs of x-ray images. An increase is detectable for the centered position. The high standard deviation reduces the validity slightly.

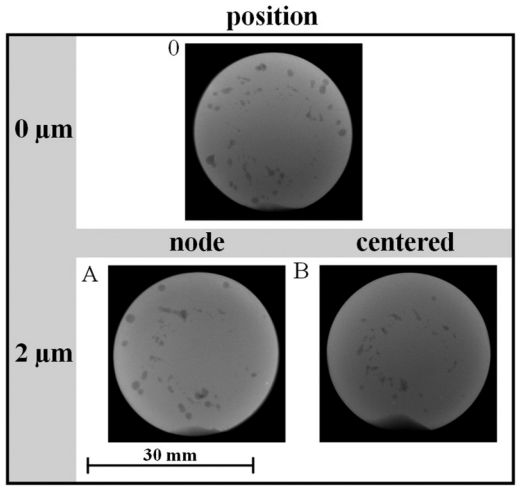

FIG. 20. Photographs of x-ray images: exemplary for parameters 0, A and B.

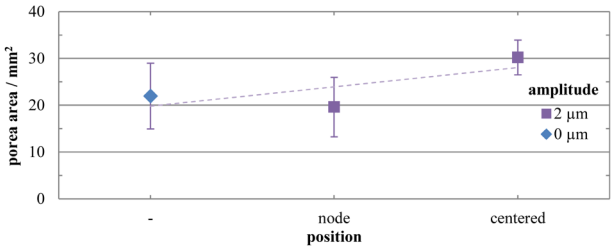

FIG. 21. Correlation between summed pore area and position and amplitude.

VI. SUMMARY

The presented bead on plate laser beam welding tests with AA6082 demonstrated the influence of ultrasonic vibration on the welding process regarding amplitude and position in the vibration distribution.

- For higher amplitudes, the grain size is more homogeneous and smaller in general and the position in the waveform of the vibration shows a grain refinement for increasing position (moving from node to antinode).
- The weld depth and weld width decrease with increasing amplitude and the width/depth ratio increases.
- The weld depth increases and the weld width decreases with increasing position (note to antinode) and the width/depth ratio decreases.
- The weld metal area is just dependent on the laser beam welding process energy.
- There is a threshold which marks the point, where the force of the ultrasonic vibration on the liquid melt is high enough to close the bottom part of the keyhole.
- Porosity area seems not to be reduced for the small sample considered here, but a change of the distribution of the porosities and travel for increasing amplitude and position movement from node to antinode to the bottom area of the weld is indicated. This suggests a worse degassing and supports the theory of the collapse of the bottom keyhole section.

VII. OUTLOOK

In further investigations, full penetration welds (half of the diameter of the round bars) are conceivable to evaluate the influence of the weld depth and define the threshold of vibration for which a keyhole formation with sufficient depth is possible.

The signals in the system were logged during the laser beam welding process, so an analysis of the data recorded could provide information about the processes in the weld metal.

The influence on the mechanical strength, primarily through the grain refinement, has to be proven. For the evaluation of the mechanical characteristics butt joints may be used, and a transfer to different materials and similar and dissimilar joints are planned.

ACKNOWLEDGMENTS

The results presented in this paper were obtained from the Collaborative Research Centre 1153 "Process chain to produce hybrid high performance components with Tailored Forming" in subproject A3. The authors would like to thank the German Research Foundation (DFG) for the financial and organizational support of this project.

REFERENCES

[1]A. San-Martin and F. D. Manchester, "The al-h (aluminum-hydrogen) system," J. Phase Equilib. **13**, 17–21 (1992).
[2]N. Seto, S. Katayama, and A. Matsunawa, "Porosity formation mechanism and suppression procedure in laser welding of aluminium alloys," Weld. Int. **15**, 191–202 (2001).
[3]J. Campbell, "Effects of vibration during solidification," Int. Met. Rev. **26**, 71–108 (1981).
[4]W. Jiang, X. Chen, B. Wang, Z. Fan, and H. Wu, "Effects of vibration frequency on microstructure, mechanical properties, and fracture behavior of A356 aluminum alloy obtained by expendable pattern shell casting," Int. J. Adv. Manuf. Technol. **83**, 167–175 (2016).
[5]A. Krajewski, W. Włosiński, T. Chmielewski, and P. Kołodziejczak, "Ultrasonic-vibration assisted arc-welding of aluminum alloys," Bull. Pol. Acad. Sci. Tech. Sci. **60**, 841–852 (2012).
[6]K. Balasubramanian, D. Kesavan, and V. Balusamy, "Studies on the effect of vibration on hot cracking and grain size in AA7075 aluminum alloy welding," Int. J. Eng. Sci. Technol. **3**, 681–686 (2011).
[7]J. S. Kim, T. Watanabe, and Y. Yoshida, "Ultrasonic vibration aided laser welding of Al alloys improvement of laser welding-quality," J. Laser Appl. **7**, 38–46 (1995).
[8]T. Radel, "Mechanical manipulation of solidification during laser beam welding of aluminum," Weld. World **62**, 29–38 (2018).
[9]P. Woizeschke, T. Radel, P. Nicolay, and F. Vollertsen, "Laser deep penetration welding of aluminum alloys with simultaneously applied vibrations," Lasers Manuf. Mater. Process. **4**, 1–12 (2017).
[10]S. Nothdurft, A. Springer, S. Kaierle, H. Ohrdes, J. Twiefel, J. Wallaschek, M. Mildebrath, H. J. Maier, T. Hassel, and L. Overmeyer, "Laser welding of dissimilar low-alloyed steel-steel butt joints and the effects of beam position and ultrasound excitation on the microstructure," J. Laser Appl. **30**, 011891 (2018).
[11]J. Twiefel, M. Klubal, M. Paiz, S. Mojrzisch, and H. Krüger, "Digital signal processing for an adaptive phase-locked loop controller," Proc. SPIE **6926**, 69260A-1 (2008).
[12]I. Ille and J. Twiefel, "Model-based feedback control of an ultrasonic transducer for ultrasonic assisted turning using a novel digital controller," Phys. Proc. **70**, 63–67 (2015).

Meet the Author

Dipl.-Ing. Sarah Nothdurft studied mechanical engineering at the Leibniz University Hannover. She joined the Department of Materials and Processes at the Laser Zentrum Hannover e.V. in 2013 as a member of Joining and Cutting of Metals group, since 2018 she is head of the Joining and Cutting of Metals group. Her main research subject is joining of similar and dissimilar materials.